BOOSTING THE MAGNETIC FIELD OF A TOROIDAL CONDUCTIVE FLUID BY A POLOIDAL FLOW

Mamoru Otsuki*

Independent researcher

ORCID: 000-0002-5878-1300

**e-mail*: gangankeisun@nifty.com

Abstract This paper demonstrates that it is possible to induce axisymmetric magnetic fields by a poloidal flow to determine the effect on the magnetic field caused by a certain flow of a conductive fluid. Using a simultaneous equation expressed by inductances induced from the induction equation expressed by a vector potential and treating the current as an eigenvalue problem, it is shown that different current modes can exist. While there are many different expressions of the electromagnetic induction equation, the use of the simultaneous equation expressed by inductances is novel. Each mode varies according to its eigenvalue, which can be positive under certain conditions, resulting in an eigenvector that increases over time, thereby maintaining a magnetic field, at least in a poloidal flow. Several case studies based on the dimensions and plasma properties of a star are reviewed; however, there are no dimensional restrictions to the provided equations, which are expected to be appropriate for various applications. For example, the proposed methodology could be applied to enhance the understanding of specific phenomena occurring in celestial bodies (planets and stars).

Keywords: Poloidal flow, dynamo theory, electromagnetic induction, inductance, conductive fluid, magnetohydrodynamics

1. INTRODUCTION

Over a century ago, Larmor hypothesized that the Sun's magnetic field may be a result of electromagnetic induction caused by the flow of an electrically conductive fluid, which is now

known as the dynamo effect [1]. The dynamo theory describes the process of magnetic field generation by self-induction in electrically conducting fluids [2]. The mechanism driving the fluid flow depends on the system; in the case of planets and stars, convection is prominent, whereas turbulence or differential rotation plays a role in other systems. The mechanism that equilibrates the magnetic field is the Lorentz force in the momentum equation, which alters the flow sufficiently to prevent it from further amplifying the field [3]. Although mainly used in astrophysics and geophysics, magnetohydrodynamic theories such as the dynamo theory are also relevant in plasma physics, metallurgy, and liquid sodium [4] experiments used to simulate the molten core of the Earth.

While dynamo theorems clarify the conditions under which dynamos can exist, there are many anti-dynamo theorems (ADTs) that specify conditions under which dynamos cannot be maintained. The first ADT was proposed by Cowling in 1934 [5]; it states that an axisymmetric magnetic field cannot be maintained by axisymmetric fluid motion [6], and non-axisymmetric modes are needed to explain the dynamo mechanism. This is known as Cowling's ADT or the axisymmetric ADT. Axisymmetric magnetic fields are generally decomposed by ohmic losses into a poloidal field and an azimuthal component. Differential rotation or other mechanisms can stretch the poloidal field, thereby converting it into an azimuthal field. This process can amplify the magnetic field when the source is a poloidal field. However, in two-dimensional geometry, the poloidal field eventually decays because there is no corresponding source. The flow of the conducting fluid is assumed to advect the poloidal field; however, because of axisymmetry, the poloidal field cannot be amplified by this mechanism [7].

This ADT has been very difficult to comprehensively prove. It was revisited relatively recently, and some open questions were answered [8]. This ADT has been considered for

stationary and dynamic systems, non-solenoid flows, variable conductivity, and other specific cases. This theorem has been well proven for many specific cases; however, the substantial complexity of magnetohydrodynamic systems implies that there may be some cases wherein the theorem does not hold. In general, the ADTs all highlight that successful dynamos have a low degree of symmetry.

In previous studies, it was assumed that axisymmetric magnetic fields do not occur with simple convection (but require aspects such as turbulence). However, this study assumes a case where this can be true. Because of the extraordinary complexity of natural and experimental systems involving conducting fluids, simplifications are made to the mathematics to enable analysis [2]. One of the most successful methods is kinematic dynamo analysis, where the types of fluid motion that can sustain a dynamo are generally investigated by solving the magnetic induction equation, often in the form of $\partial_t B = R_m \nabla \times (u \times B) + \nabla^2 B$. Here, B is the magnetic flux density, u is the velocity, and R_m is the magnetic Reynolds number of the conductive fluid, which quantifies the effectiveness of the fluid motion in amplifying the magnetic field against decay due to electrical resistance [9]. Many different induction equations have been presented. These have been modified depending on the specific boundary conditions, geometry, scale, etc., of the system of interest.

To the best of the author's knowledge, most theoretical treatments express the electromagnetic induction formula in terms of B (or the magnetic field strength, H). However, the novelty of this study is that the induction formula is expressed in terms of the inductance. Thus, the current and vector potential can be expressed as toroidal coils, making it easier to observe the behavior of the current mode (as eigenvectors). Furthermore, the vector potential can be replaced by the inductance, enabling calculations using a common expression for the inductance. The

presented theory is expected to be useful for studying magnetic field generation in systems with various sizes and flow velocities. However, case studies assuming the dimensions and plasma conductivity of the Sun are used as examples. Other relevant topics could include planetary systems, plasma furnaces, and liquid sodium experiments.

2. MECHANISM

2.1 Description of the problem

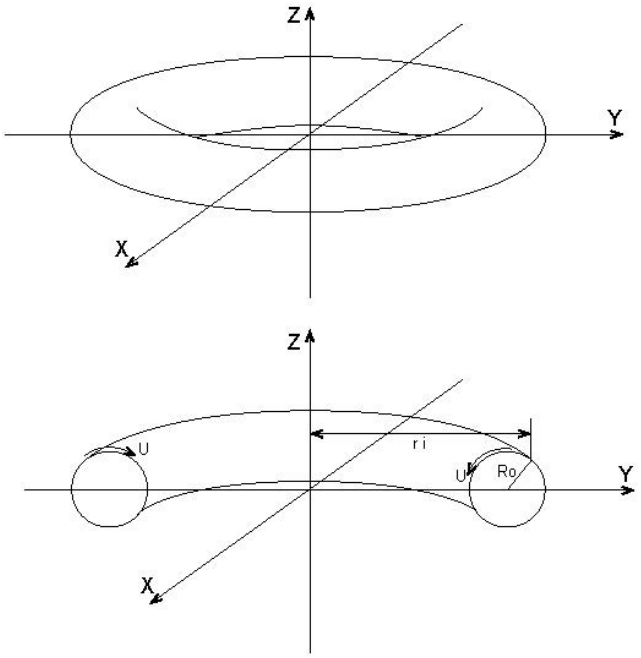

Fig. 1. Schematic of the toroidal geometry.

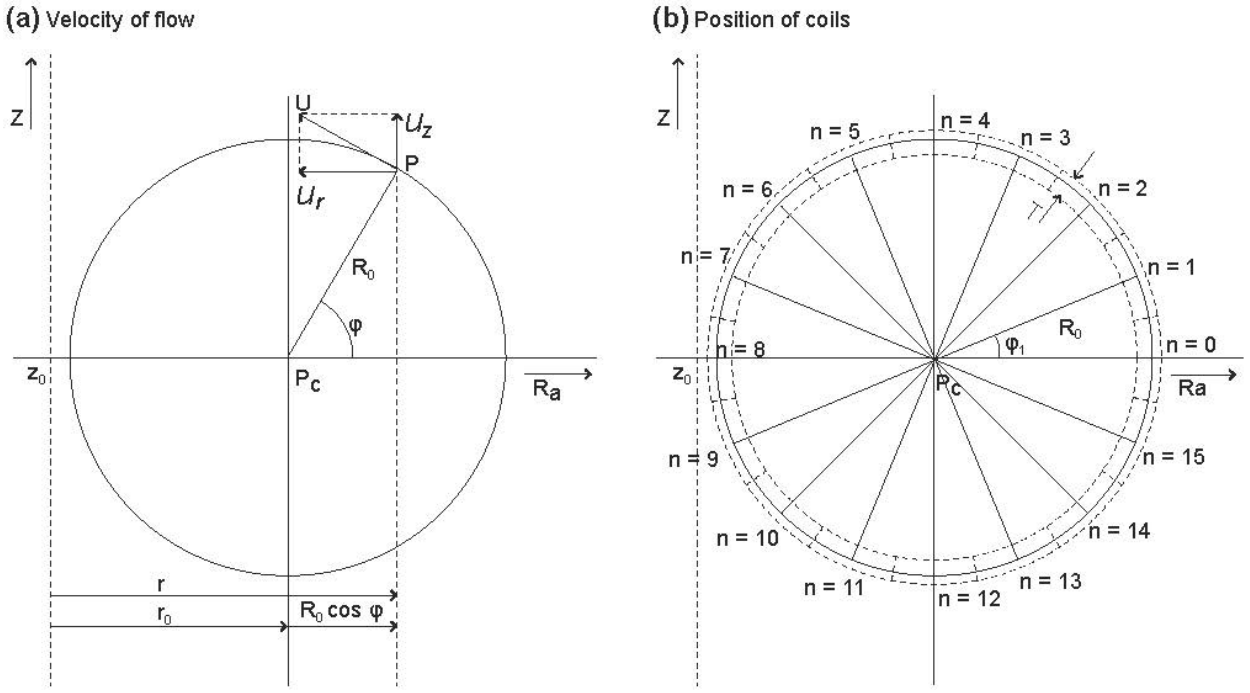

Fig. 2. Schematics of the (a) velocity of the fluid flow and (b) defined coils in the cross-section of convection (Y–Z plane in Fig. 1).

To determine whether a magnetic field can fluctuate in the poloidal stream of a conductive fluid, a certain poloidal flow is set, and the induction equation (as a simultaneous equation expressed by inductances) is expressed in terms of toroidal vector potentials to calculate the current as an eigenvalue problem. The poloidal flow of a fluid occurs in a torus shape, as shown in Fig. 1, where U is the poloidal velocity, R_0 is the radius of the poloidal flow, and r_i is the radius of an example point on the torus from the Z axis. A representative cross-section of the torus (Y–Z plane in Fig. 1) is shown in Fig. 2(a). The stream is divided into toroidal segments for calculation as coils (Fig. 2(b)). In this figure, Z is the center axis, and Ra is the radial axis of the cylindrical coordinates (equivalent to the Y axis in Fig. 1), where the circle indicates the cross-section of the torus. P_c is the center of the flow, where r_0 and z_0 are the elements of P_c in the Ra and Z directions, respectively. Note that z_0 is at the coordinates (0,0) and P_c is at (r_0,0). In Fig. 2(a), P is a

representative position at which flow velocity vector U is calculated; u_r and u_z are elements of U in the Ra and Z directions, respectively; φ is an angle between the Ra axis and point P; and r is the element of P in the Ra direction. Fig. 2(b) shows the definition of the coils used to define the flow torus. Sixteen coils are considered, where n refers to the coil number. The dotted lines indicate the coaxial coils (i.e., the region occupied by the fluid), which are separated by thickness T. There are multiple coils that wind only once around the Z axis, and the coils move in the direction of U with radius R_0. Electric current runs separately in each coil in the θ direction. Although the coils can move, the later calculation of the eigenvalues assumes the state of the coils in a brief moment, Δt.

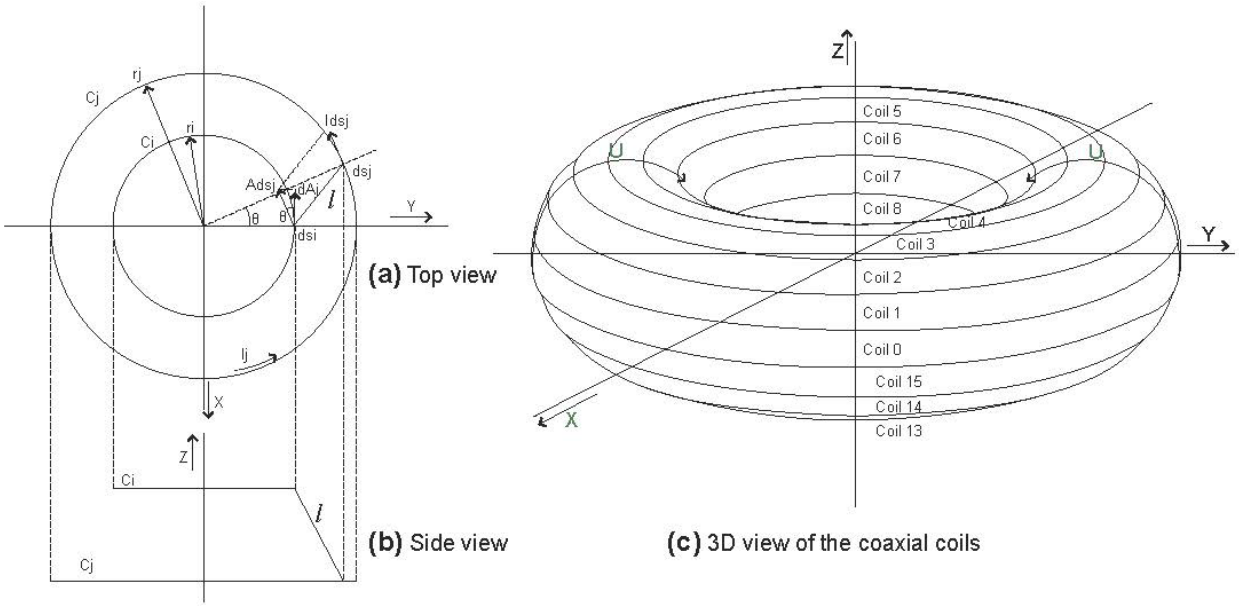

Fig. 3. Relationship between the electric current (I) and vector potential (A) for a set of any two coils shown in Fig. 2: (a) top view and (b) side view of the torus, and (c) 3D view of the coaxial coils.

Figs. 3(a) and (b) show the top and side views, respectively, of a set of any two of the coaxial coils shown in Fig. 2 to explain the relationship between the electric current (I) and vector potential (A). In addition, Fig. 3(c) shows a 3D image of the coils to clarify their relationship with each

other. Each coil is arrayed coaxially with the Z axis, and they are parallel to each other. X, Y, and Z are the axes of the rectangular Cartesian coordinate system shown in Fig. 3. C_j is coil j, which has current I_j, and C_i is coil i, which obtains vector potential A_j induced by current I_j running in coil C_j. θ is the angle of rotation around the Z axis, starting from the Y axis. Here, r_i and r_j are the radii of C_i and C_j, respectively. Furthermore, ds_i and ds_j are minute lengths of C_i and C_j for integration, respectively, where ds_i is placed on the X axis ($\theta = 0$), and ds_j is placed at θ with distance $\boldsymbol{l}$ between them to define the range of the integral. Ids_j is the contribution to the current over ds_j, where Ads_j is the vector potential induced by Ids_j. dA_j is the element of Ads_j in the X direction, and it is integrated with respect to θ to give A_j. Φ_i is the total flux linking C_i.

2.2 Calculation of the magnetic properties

To determine the fluctuation in the magnetic field in the coils described in the previous section, the current is calculated using a presentation of Ohm's law that includes the electric field [10].

$$J = \sigma(E + u \times B) \tag{1}$$

Here, J is the current density; σ is the electric conductivity; u is the velocity of the conductive fluid; and B is the magnetic field, which can be found using Eq. (2); $u \times B$ is the motion of the electric field; and E is the electric field potential, which can be found using Eq. (3).

$$B = \nabla \times A \tag{2}$$

$$E = -\frac{\partial A}{\partial t} + \nabla\varphi' \tag{3}$$

Here, φ' is a scalar potential, A is a vector potential, and t is time.

To derive an induction equation expressed in vector potentials from Ohm's law, these equations are combined as follows.

$$\frac{\partial A}{\partial t} - u \times (\nabla \times A) = \nabla \varphi' - \frac{J}{\sigma} \quad (4)$$

To apply this induction equation for coils, the factor $2\pi r$ (r = coil radius) is multiplied as an integral around the coil on both sides of the equation because the current is the same around C_j. Assuming $J = I/S$, where I is the toroidal current and S is the cross-sectional area of the coil, then Eq. (4) is rewritten as follows.

$$\frac{\partial}{\partial t}(2\pi r_i A) - u \times (\nabla \times 2\pi r_i A) = -\frac{2\pi r_i}{\sigma}\frac{I}{S} \quad (5)$$

Here, φ' is ignored because it is assumed that the conductivity of the fluid is high. Furthermore, Eq. (6) shows the relationship between A and the inductance (L) [11]. Here, the total magnetic flux linking the coil, Φ, is used in place of L, where $\Phi = LI$. The subscripts i and j refer to the coil numbers defined in Fig. 2, enabling the development of simultaneous equations.

$$\Phi_i = \oint_{C_i} A_j ds_i \quad (6)$$

Here, Φ_i is the flux of coil C_i, and ds_i is a minute part of coil C_i.

In this arrangement of coils, all the coils are arrayed coaxially with the Z axis and parallel to each other. Thus, A_j is the same around C_i. Therefore, $\Phi_i = 2\pi r_i A_j$ when $\Phi_i = L_{ij} I_j$. Then, the relationship between L_{ij} and A_j is as follows. L_{ij} is a matrix meaning inductance, but only the diagonal element is self-inductance, and the other elements are mutual inductance, so it is hereafter referred to as M_{ij}.

$$A_j = \frac{I_j}{2\pi r_i} M_{ij} \tag{7}$$

By substituting Eq. (7) into Eq. (5), the following equation is obtained.

$$\frac{\partial}{\partial t}\left(M_{ij} I_j\right) - u_i \times \left(\nabla \times 2\pi r_i A_j\right) = -\frac{2\pi r_i}{\sigma S} I_j \tag{8}$$

Here, σ is the conductance of the fluid, and r_i is the radius from the Z axis. However, the second term on the left-hand side of Eq. (8) is complicated. Thus, it must be dealt with separately. It is considered by decomposing the term as follows.

$$u_i \times \left(\nabla \times A_j\right) = \begin{bmatrix} u_{ir} \\ 0 \\ u_{iz} \end{bmatrix} \times \begin{bmatrix} \frac{1}{r_i}\left(-r_i \frac{\partial A_{j\theta}}{\partial z_i}\right) \\ 0 \\ \frac{1}{r_i}\left(\frac{\partial r_i A_{j\theta}}{\partial r_i}\right) \end{bmatrix} = \begin{bmatrix} u_{ir} \\ 0 \\ u_{iz} \end{bmatrix} \times \begin{bmatrix} -\frac{\partial A_{j\theta}}{\partial z_i} \\ 0 \\ \frac{1}{r_i} A_{j\theta} + \frac{\partial A_{j\theta}}{\partial r_i} \end{bmatrix} =$$

$$\begin{bmatrix} 0 \\ -u_{iz} \frac{\partial A_{j\theta}}{\partial z_i} - u_{ir}\left(\frac{1}{r_i} A_{j\theta} + \frac{\partial A_{j\theta}}{\partial r_i}\right) \\ 0 \end{bmatrix} \tag{9}$$

Here, rotA_j is decomposed into cylindrical coordinates, and subscripts r, θ, and z indicate the component directions in cylindrical coordinates, namely, the radius from the Z axis, angular around the Z axis, and Z direction, respectively. A_j has a component only in the θ direction. Thus, the other components of A_j are omitted. Eq. (10) is obtained by multiplying Eq. (9) by $2\pi r_i$, substituting Eq. (7) and including only the θ component.

$$2\pi r_i \left[-u_{iz} \frac{\partial A_{j\theta}}{\partial z_i} - u_{ir}\left(\frac{1}{r_i} A_{j\theta} + \frac{\partial A_{j\theta}}{\partial r_i}\right)\right] = -u_{iz} \frac{\partial M_{ij} I_{j\theta}}{\partial z_i} - u_{ir}\left(\frac{1}{r_i} M_{ij} I_{j\theta} + \frac{\partial M_{ij} I_{j\theta}}{\partial r_i}\right)$$

$$= -u_{ir} \frac{\partial M_{ij} I_{j\theta}}{\partial r_i} - u_{iz} \frac{\partial M_{ij} I_{j\theta}}{\partial z_i} - u_{ir} \frac{1}{r_i} M_{ij} I_{j\theta} \tag{10}$$

This is replaced by the second term on the left-hand side of Eq. (8) to obtain Eq. (11).

$$\frac{\partial}{\partial t}\left(M_{ij}I_{j\theta}\right) - \left(-u_{ir}\frac{\partial M_{ij}I_{j\theta}}{\partial r_i} - u_{iz}\frac{\partial M_{ij}I_{j\theta}}{\partial z_i} - u_{ir}\frac{1}{r_i}M_{ij}I_{j\theta}\right) = -\frac{2\pi r_i}{\sigma S}I_{j\theta} \tag{11}$$

$$\frac{\partial}{\partial t}\left(M_{ij}I_{j\theta}\right) + u_{ir}\frac{\partial M_{ij}I_{j\theta}}{\partial r_i} + u_{iz}\frac{\partial M_{ij}I_{j\theta}}{\partial z_i} + u_{ir}\frac{1}{r_i}M_{ij}I_{j\theta} = -\frac{2\pi r_i}{\sigma S}I_{j\theta} \tag{12}$$

Since the first three terms on the left-hand side of Eq. (12) are equivalent to a total differential, they can be replaced as follows:

$$\frac{d}{dt}\left(M_{ij}I_{j\theta}\right) + u_{ir}\frac{1}{r_i}M_{ij}I_{j\theta} = -\frac{2\pi r_i}{\sigma S}I_{j\theta}$$

$$\frac{dM_{ij}}{dt}I_{j\theta} + M_{ij}\frac{dI_{j\theta}}{dt} + u_{ir}\frac{1}{r_i}M_{ij}I_{j\theta} = -\frac{2\pi r_i}{\sigma S}I_{j\theta}$$

$$\frac{dI_{j\theta}}{dt} = {M_{ij}}^{-1}\left(-\frac{dM_{ij}}{dt}I_{j\theta} - u_{ir}\frac{1}{r_i}M_{ij}I_{j\theta} - \frac{2\pi r_i}{\sigma S}I_{j\theta}\right)$$

$$\Lambda I_{j\theta} = -{M_{ij}}^{-1}\frac{dM_{ij}}{dt}I_{j\theta} - {M_{ij}}^{-1}u_{ir}\frac{1}{r_i}M_{ij}I_{j\theta} - {M_{ij}}^{-1}R_{ij}I_{j\theta} \tag{13}$$

Here, Λ indicates the eigenvalues. These simultaneous equations are used here to obtain the Λ values. R_{ij} is a matrix of resistance, and a function of the coil's circumference and cross-sectional area S, where S is calculated from the thickness T and the section of the flow course as $S = (2\pi R_0 T)/16$. Then, $R_{ij} = 2\pi r_i/(\sigma S) = (16 r_i)/(\sigma R_0 T)$. R_{ij} is a diagonal matrix because the voltage drop exists only for $i = j$.

In the coil description shown in Fig. 2, the coil's cross-sectional area and shape are disregarded in the calculation of the inductance because these geometrical factors introduce a large degree of complexity. Therefore, the coil is treated as a thin line as an approximation in Fig. 3(a) and (b). Subsequently, A_j is calculated as follows [10]:

$$A_j = \frac{\mu}{4\pi}\oint_{C_j}\frac{J}{l}dV = \frac{\mu}{4\pi}\oint_{C_j}\frac{JS}{l}ds_j = \frac{\mu}{4\pi}\oint_{C_j}\frac{I_j}{l}\cos\theta\, ds_j = \frac{\mu}{4\pi}I_j\oint_{C_j}\frac{\cos\theta}{l}ds_j, \tag{14}$$

where l is the distance between ds_i and ds_j, μ is the magnetic permeability, dV is the minute volume, S is the cross-sectional area of the current (i.e., the coil), $I_j = JS$ is the current, and the directional element for ds_i of I_j is $I_j \cos\theta$. When Eq. (7) is substituted for A_j in Eq. (14). Eq. (15) is obtained.

$$M_{ij} = \frac{2\pi r_i}{I_j}\frac{\mu}{4\pi} I_j \oint_{C_j} \frac{\cos\theta}{l} ds_j = 2\pi r_i \frac{\mu}{4\pi} \oint_{C_j} \frac{\cos\theta}{l} ds_j \quad (15)$$

When μ is set to $4\pi \times 10^{-7}$ H/m (vacuum conditions), Eq. (16) is obtained.

$$M_{ij} = 2\pi r_i \oint_{C_j} \frac{\cos\theta}{l} ds_j \times 10^{-7} \quad (16)$$

M_{ij} is calculated by summation, where C_j is divided into $k = 100$ equal parts, Δs_j, as follows.

$$M_{ij} \fallingdotseq 2\pi r_i \sum_{k=1}^{100} \frac{\cos\theta_k \Delta s_j}{l_k} \times 10^{-7} \quad (17)$$

$$l_k = \sqrt{(r_n \cos\theta_k - r_{n'})^2 + (r_n \sin\theta_k)^2 + (z_n - z_{n'})^2} \quad (18)$$

The angle of a specific coil, n, is given by $\varphi_n = 2\pi n/16$, as shown in Fig. 2, where $r_n = r_0 + R_0\cos\varphi_n$ and $z_n = R_0\sin\varphi_n$. Here, n' is another coil number. Earlier, i and j were used in the mutual inductance calculations to distinguish between coils that received electromotive force and coils that had a current flow. However, in this case, n and n' are any two of the coils. Here, $\dot{(\ )}$ is the same as $\frac{d}{dt}$ below. $\dot{M}_{ij}$ is calculated as the difference in M_{ij} induced by the flow velocity over a period of a minute, divided by Δt (1.0×10^{-6} s). The velocity U shown in Fig. 2 depends on the φ_n of each coil and is calculated as follows:

$$|U| = \omega R_0, u_r = -|U|\sin\varphi_n,\ u_z = |U|\cos\varphi_n, \quad (19)$$

where ω is the angular velocity of the flow. Furthermore, M_{ij}^{-1} is the inverse matrix of M_{ij}.

3. RESULTS AND DISCUSSION

Here, several eigenvalue case studies are described based on Eq. (13), as presented in the previous section. Four different cases are defined, as shown in Table 1. Table 2 lists the eigenvalues (Λ_1–Λ_{16}). Positive values contribute to the eigenvector increasing over time, while negative values make it decrease over time. The positive values are highlighted in bold in the table. The general conditions assumed in the calculations of the eigenvalues were $\sigma = 1.0 \times 10^4$ S/m (based on typical plasma conductivity [12]) and T=0.1R_0.

In the case of condition 1, Λ_{16} is the Λ value with the largest positive value, which implies that the eigenvector increases in magnitude over time. The number of positive eigenvalues depends on the size of the system and the flow velocity. Therefore, in the case of condition 2 (with a higher ω than condition 1 but the same system dimensions), five of the Λ values are positive. Therefore, increasing the flow velocity causes the eigenvector magnitude to increase over time. In the case of condition 3, with a lower ω but the same dimensions as condition 1, all the Λ values are negative. Therefore, the eigenvector would only decrease, and the magnetic field would not be sustained over time. In the case of condition 4, the dimensions are a magnitude larger than those for condition 1. Because ω is an angular velocity, it scales proportionally. Thus, ω was decreased accordingly by an order of magnitude to make it comparable with condition 1. In this case, five of the Λ values are positive. Therefore, it is easier to increase the eigenvector over time (i.e., maintain a magnetic field) for larger systems.

Note that Eq. (13) implies that the $-{M_{ij}}^{-1}\dot{M}_{ij}I_{j\theta}$ term may become positive (i.e., $\dot{M}_{ij}$ becomes negative) because $\dot{M}_{ij}$ depends on the velocity of the fluid. Therefore, the eigenvalue (Λ)

is also dependent on the velocity, and some of the eigenvalues may be positive, i.e., eigenvectors that grow over time. The inductance has no effect on the $-{M_{ij}}^{-1}u_{ir}\frac{1}{r_i}M_{ij}I_{j\theta}$ term because ${M_{ij}}^{-1}$ and M_{ij} almost cancel each other out. However, the velocity of the radius vector of coil *i* (u_{ir}), i.e., the speed of convection, depends on the coil position. Therefore, this term is positive if the velocity is negative. However, according to the calculations, the effect is negligible. In addition, the $-{M_{ij}}^{-1}R_{ij}I_{j\theta}$ term is always negative and implies the attenuation of the eigenvalue. The inductance M_{ij} in Eq. (15) is proportional to R_0 and r_0 because r_i, l, and ds originate from R_0 and r_0. Furthermore, R_{ij} is inversely proportional to R_0 and r_0 because in the equation $R_{ij} = (16r_i)/(\sigma R_0 T)$, R_0, T, and r_i originate from and are inversely proportional to R_0 and r_0. Then, these terms are included in the $-{M_{ij}}^{-1}R_{ij}I_{j\theta}$ term. Larger systems imply that the eigenvectors are less likely to attenuate. This is clearly indicated by the results for the four presented conditions. When the inductance of coils changes by the flow velocity, the eigenvalues determined from the simultaneous equations (13) enable the interaction between changes in coil inductance, and resistance to be shown as a fluctuation in the toroidal current, which means a fluctuating magnetic field.

Some eigenvalues become positive under certain conditions, indicating that their eigenvector would increase over time. A positive eigenvalue increases its eigenvector (current mode that means each current of coils but note that the current is not determined by its absolute value and polarity because of the character of their eigenvector) exponentially. In contrast, a negative eigenvalue decreases its eigenvector exponentially. A decrease only occurs if there is a current mode corresponding to the existing negative eigenvalue, regardless of the magnitude of the negative eigenvalue. Of course, this is only true in a case where each eigenvector is orthogonal.

This calculation does not show perfect orthogonality; if the matrix on the right-hand side of Eq. (13) is separated into symmetric and alternating components, and the latter is not zero, indicating imperfect orthogonality. However, this is attributable to the coarse calculation. As a potential future work, numerical calculations are necessary to increase the order of the matrix and set the convection current over a wide area to evaluate the orthogonality of this system. However, this was beyond the scope of this theoretical contribution. Notably, even if the orthogonality is not perfect, the positive eigenvalues are expected to have some influence on the generated magnetic field. In the case of the large number of positive eigenvalues calculated in this study, it is expected that they would be dominant and increase the current eigenvector. The eigenvector of a negative eigenvalue is only influential if there is a current generated by the eigenvector of a positive eigenvalue. This can suppress the eigenvector with the positive eigenvalue but cannot reduce it to zero. Therefore, it is expected that the increasing trend in the eigenvector would be sustained by the positive eigenvalues, and the extent of this would depend on the specific conditions.

It is assumed that the balance between the first (current-induced inductance change) and third (loss-induced ohmic losses) terms on the right side is included in Eq. (13). The changes in the inductance and current terms are separated, and the inductance terms end up on the right-hand side of the equation, which is one of the reasons why the right-hand side of this equation and eigenvalues can be positive. Other theories do not have this viewpoint. Farrell and Ioannou also used an eigenvalue description of an electromagnetic induction equation (expressed in terms of B); however, only negative eigenvalues were observed [13]. The theoretical analysis provided here proposes that a poloidal axisymmetric magnetic field is generated by the poloidal flow of a fluid. As another important difference, many previous studies assumed that the magnetic field was generated as a result of turbulence [14], while I show here that this condition is not necessary. To

the best of the author's knowledge, this is a novel idea, and there have been no other studies that calculated specific eigenvalues and showed how the magnetic field generation changed with the velocity of the fluid and the size of the system.

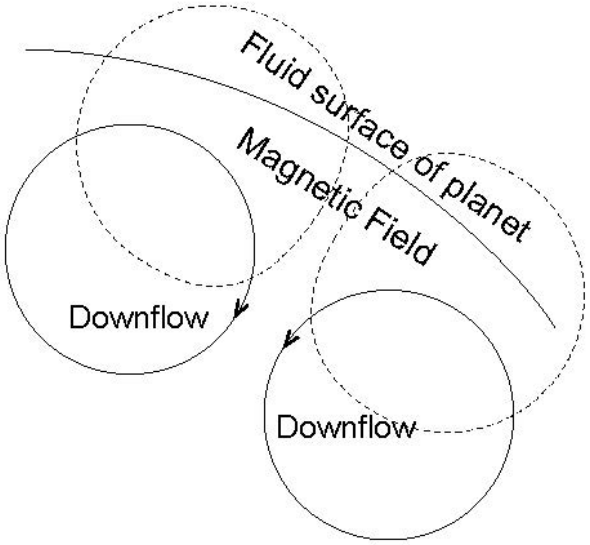

Fig. 4. Examples of poloidal axisymmetric convection in a celestial body. The solid arrows indicate the fluid flow, while the dashed lines indicate the induced magnetic field.

The methodology presented here is relevant for conditions where a poloidal axisymmetric magnetic field is generated. In the conductive fluid of a celestial body, poloidal convection may occur as a result of downflow due to a radial temperature gradient or chemical effects, as shown in Fig. 4. The Sun and Earth have poloidal axisymmetric magnetic fields. However, mainly the generation mechanism is different from that assumed here. While this mechanism probably includes that described here by the presented theory, for the moment, it is probably indistinguishable because it is mixed. In the liquid sodium experiments used to model the Earth's core [4], it is difficult to obtain a smooth flow velocity, which is one of the assumptions made here.

In other words, because convection is generated by a propeller in this system now, the flow is disturbed, and the magnetic field generation described here is unlikely to occur.

In another example, in a plasma reactor, if such convection is generated, a magnetic field is added in addition to the external magnetic field. Because a strong magnetic field is applied externally, the magnetic field generated by the fluid flow is also probably indistinguishable, and depending on the conditions, it may not occur. Moreover, this reactor is also too small, which is disadvantageous for this mechanism. Because it has been assumed that these magnetic fields are not generated in such systems, researchers may not have specifically looked for them for the moment.

This paper shows calculations for a specific fluid flow (a thin layer of fluid under poloidal flow). The convection used in this paper is intended to provide a calculation example. If you know realistic convection, you can calculate it with that convection. Since the flow velocity can be set at any position, it is not necessary to be convection in a thin region such as the convection shown here. In other words, in the case of axisymmetric poloidal convection, it is possible to calculate by setting the convection distributed in an arbitrary region. Furthermore, it may not be circulating convection.

To apply this theory to real systems, it is necessary to consider the dynamics with respect to the Lorentz force and other factors [15]. To demonstrate the possibility and magnitude of magnetic field generation as a function of the size and flow velocity of the system, the scale of the Sun and its corresponding plasma conductivity were assumed here as a representative example.

However, the mathematics presented in this paper will be useful in the Sun, Earth and other celestial bodies, plasma furnaces, and sodium experiments in the future.

Conflicts of interest.

The author has no conflicts of interest to declare.

Funding.

No funding was obtained for this work.

Acknowledgements

Editorial support, in the form of writing, assembling tables, creating high-resolution images based on detailed directions by the author, collating the author's comments, copyediting, fact checking, and referencing, was provided by Editage, Cactus Communications.

REFERENCES

1. J. Larmor, Reports Br. Assoc. **87**, 159–160 (1919).
2. H. K. Moffat, *Field Generation in Electrically Conducting Fluids*. Cambridge University Press (1978).
3. G. Rüdiger, R. Hollerbach, *The Magnetic Universe*. First Edition. Wiley-VCH, Weinheim, Germany (2004).
4. M. M. Adams, D. R. Stone, D. S. Zimmerman, and D. P. Lathrop, Prog. Earth Planet. Sci. **2**, 1–18 (2015).
5. T. G. Cowling and Q. J. Mech. Appl. Math. **10**(1), 129–136 (1957).
6. P. H. Roberts and G. A. Glatzmaier, Rev. Mod. Phys. **72**(4), 1081–1123 (2000).
7. A. Brandenburg, Astrophys. J. **465**(2), L115-118 (1996).
8. R. Kaiser and A. Tilgner, SIAM J. Appl. Math. **74**(2), 571–597 (2014).
9. J. J. Love, Geophys. Res. Lett. **23**(8), 857–860 (1996).
10. H. S. Reall, Mathematical Tripos Part IB: Electromagnetism [Internet]. Available from: www.damtp.cam.ac.uk/user/hsr1000/electromagnetism_lectures.pdf. Accessed 03/11/2022.
11. H. A. Haus and J. R. Melcher, *Vector Potential and the Boundary Value Point of View*. In: Electromagnetic Fields and Energy [Internet], Massachusetts Institute of Technology (1998). Available from: https://ocw.mit.edu/courses/res-6-001-electromagnetic-fields-and-energy-spring-2008/pages/chapter-8/. Accessed 03/11/2022.
12. A. Kanzawa, Netsu Bussei. **4**(1), 3-11 (1990) (In Japanese).
13. B. F. Farrel and P. J. Ioannou, Astrophys. J. **522**(2), 1079–1087 (1999).
14. K. H. Burrell and J. D. Callen, Phys. Plasmas **28**(6), 1–28 (2021).
15. R. Stieglitz, Nonlin. Proc. Geophys. **9**, 165–170 (2002).

TABLES

Table 1. Definitions of the case conditions

Condition	R_0 **(m)**	r_0 **(m)**	Ω **(rad/s)**
1	1×10^3	1.1×10^3	$2\pi(16\times10^{-5})$
2	1×10^3	1.1×10^3	$2\pi(16\times10^{-4})$
3	1×10^3	1.1×10^3	$2\pi(8\times10^{-5})$
4	1×10^4	1.1×10^4	$2\pi(16\times10^{-6})$

Table 2. Eigenvalues of the four conditions shown in Table 1.

Eigenvalue	**Condition 1**	**Condition 2**	**Condition 3**	**Condition 4**
Λ_1	-2.081×10^{-2}	-4.893×10^{-2}	-2.081×10^{-2}	-4.893×10^{-4}
Λ_2	-1.589×10^{-2}	-4.017×10^{-2}	-1.587×10^{-2}	-4.017×10^{-4}
Λ_3	-1.270×10^{-2}	-2.888×10^{-2}	-1.264×10^{-2}	-2.888×10^{-4}
Λ_4	-1.052×10^{-2}	-2.184×10^{-2}	-1.037×10^{-2}	-2.184×10^{-4}
Λ_5	-9.129×10^{-3}	-2.114×10^{-2}	-8.729×10^{-3}	-2.114×10^{-4}
Λ_6	-9.030×10^{-3}	-1.821×10^{-2}	-7.562×10^{-3}	-1.821×10^{-4}
Λ_7	-8.410×10^{-3}	-1.526×10^{-2}	-6.953×10^{-3}	-1.526×10^{-4}
Λ_8	-7.465×10^{-3}	-1.155×10^{-2}	-6.656×10^{-3}	-1.155×10^{-4}
Λ_9	-6.284×10^{-3}	-7.354×10^{-3}	-5.903×10^{-3}	-7.354×10^{-5}
Λ_{10}	-5.043×10^{-3}	-4.669×10^{-3}	-4.974×10^{-3}	-4.669×10^{-5}
Λ_{11}	-4.669×10^{-3}	-2.654×10^{-3}	-4.669×10^{-3}	-2.654×10^{-5}
Λ_{12}	-3.812×10^{-3}	$\mathbf{2.815\times10^{-3}}$	-4.036×10^{-3}	$\mathbf{2.815\times10^{-5}}$
Λ_{13}	-2.624×10^{-3}	$\mathbf{9.702\times10^{-3}}$	-3.189×10^{-3}	$\mathbf{9.702\times10^{-5}}$
Λ_{14}	-1.473×10^{-3}	$\mathbf{1.908\times10^{-2}}$	-2.556×10^{-3}	$\mathbf{1.908\times10^{-4}}$
Λ_{15}	-4.744×10^{-4}	$\mathbf{3.120\times10^{-2}}$	-2.013×10^{-3}	$\mathbf{3.120\times10^{-4}}$
Λ_{16}	$\mathbf{5.746\times10^{-4}}$	$\mathbf{4.011\times10^{-2}}$	-8.293×10^{-4}	$\mathbf{4.011\times10^{-4}}$